



Hierarchical domains in Na_{1/2}Bi_{1/2}TiO₃ single crystals: Ferroelectric phase transformations within the geometrical restrictions of a ferroelastic inheritance

Jianjun Yao, Wenwei Ge, Liang Luo, Jiefang Li, D. Viehland, and Haosu Luo

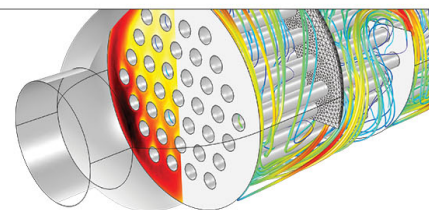
Citation: [Applied Physics Letters](#) **96**, 222905 (2010); doi: 10.1063/1.3443717

View online: <http://dx.doi.org/10.1063/1.3443717>

View Table of Contents: <http://scitation.aip.org/content/aip/journal/apl/96/22?ver=pdfcov>

Published by the [AIP Publishing](#)

Over **700** papers &
presentations on
multiphysics simulation



VIEW NOW ►

 COMSOL

Hierarchical domains in $\text{Na}_{1/2}\text{Bi}_{1/2}\text{TiO}_3$ single crystals: Ferroelectric phase transformations within the geometrical restrictions of a ferroelastic inheritance

Jianjun Yao,¹ Wenwei Ge,^{1,a)} Liang Luo,¹ Jiefang Li,¹ D. Viehland,¹ and Haosu Luo²

¹Department of Materials Science and Engineering, Virginia Tech, Blacksburg, Virginia 24061, USA

²Shanghai Institute of Ceramics, Chinese Academy of Sciences, Shanghai 201800, People's Republic of China

(Received 25 September 2009; accepted 13 May 2010; published online 3 June 2010)

We have found unique hierarchical domains in $\text{Na}_{1/2}\text{Bi}_{1/2}\text{TiO}_3$ single crystals. A tetragonal ferroelastic domain structure is unchanged on cooling from 520 to 25 °C. Polar microdomains then nucleated on cooling in the rhombohedral ferroelectric phase within the geometrical restrictions imposed by the inherited ferroelastic domains. © 2010 American Institute of Physics.

[doi:10.1063/1.3443717]

Environmental friendly Pb-free piezoelectrics have been the topic of research in the past number of years.^{1,2} One important materials system with promise is $\text{Na}_{1/2}\text{Bi}_{1/2}\text{TiO}_3$ or NBT, which was originally reported by Smolenskii,³ and which more recently has been shown to have relatively promising piezoelectric properties.^{2,4} In fact, longitudinal piezoelectric constants of $d_{33} \approx 500$ pC/N have been reported both under large amplitude drive in the ϵ -E response² and more recently under weak-field drive using a Berlincourt-type meter.⁴

The phase transformational sequence on cooling for NBT has been reported to be cubic(C) \rightarrow tetragonal(T) \rightarrow rhombohedral(R).⁵⁻⁹ with phase transition temperatures of about 520 °C and 260 °C, respectively. Interestingly, no distinct structural changes associated with the ferroelectric transformation have been reported at the maximum in the dielectric constant $T_{\text{max}} = 330$ °C.^{10,11} It would thus appear that the high temperature (paraelectric) prototypic phase of NBT has tetragonal symmetry, rather than cubic. Ferroelastic domains¹² and a splitting of the lattice parameters⁶ have been reported to persist on heating until near 520 °C, indicating that this high temperature paraelectric tetragonal phase is ferroelastic. Below T_{max} , the tetragonal phase becomes polar, where it has been reported to have double P-E hysteresis loops indicative of antiferroelectric ordering.^{1,12} Furthermore, the ferroelectric $T \rightarrow R$ transition is diffused, as evidenced by temperature dependent dielectric constant measurements.^{1,6,10} An inflection in the dielectric constant near 250 °C has been assumed to be that of the $T \rightarrow R$ transition, below which relaxor ferroelectric characteristics became evident in the dielectric constant on further cooling. Vakhrushev *et al.*⁶ have conjectured that ferroelectric rhombohedral clusters gradually form within the polar tetragonal matrix over a broad temperature range on cooling between 330 and 200 °C.

Relaxor ferroelectrics, such as $\text{Pb}(\text{Mg}_{1/3}\text{Nb}_{2/3})\text{O}_{3-x}\%$ PbTiO_3 or $\text{PMN-x}\%$ PT , are characterized by the presence of polar clusters as observed by electron microscopy.¹³ With increasing x, piezoforce microscopy (PFM) and polarized light microscopy (PLM) investigations have shown^{14,15} that these polar nanoregions self-assemble

into small domain striations along the $\langle 110 \rangle$ that are submicron sized, which subsequently geometrically organize into large $\{100\}$ platelets or bands of about 100 μm in size. These hierarchical domain organizations are similar to those of martensite^{16,17} where such arrangements achieve stress accommodation relaxing the elastic energy. However, in spite of the relaxor analogy for the R phase of NBT, neither the presence of polar nanoregions nor hierarchical domains has yet been reported.

Here, we have studied the phase transformation and domain structures of NBT by a variety of structural and microstructural methods. We find (i) that the high temperature tetragonal ferroelastic domain structure is unchanged on cooling from 520 to 25 °C, where it is elastically inherited by the ferroelectric rhombohedral phase; and (ii) that polar microdomains nucleate on cooling in the rhombohedral ferroelectric phase, tending to self-organize to a limited extent along $\langle 110 \rangle$. These results reveal a unique presence of independent ferroelastic and ferroelectric domain structures.

Single crystals of NBT were grown by a top-seeded solution growth method.¹⁸ $\langle 001 \rangle$ oriented wafers of NBT single crystals were cut into dimensions of $5 \times 5 \times 0.5$ mm³, and the surfaces were polished down to a 0.25 μm finish. Careful investigations of the domain structure were performed by SPM using Piezoforce (Vecoo DI 3100a) and Raman (Witec Alpha500) modes; and by PLM using a Leica Microsystem (Wetzlar GmbH) equipped with a hot stage. Temperature dependent lattice parameters were determined by x-ray diffraction (XRD) using a Philips MPD high-resolution system equipped with a doomed hot-stage. The x-ray wavelength was that of Cu $K_{\alpha} = 1.5406$ Å. The dielectric constant was measured as a function of temperature using a LCR meter (HP 4284). For these measurements, silver electrodes were coated on the major surfaces.

Figure 1(a) shows the temperature dependent dielectric data. In this figure, we can see that the dielectric maximum occurs near 330 °C, near and just below which the dielectric constant is frequency independent. On further cooling, an inflection was found near 250 °C below which notably frequency dispersion was observed. This dispersion was similar to that of relaxors below T_{max} ,¹⁹ indicating polar heterogeneities with low frequency fluctuations. In Fig. 1(b), temperature dependent lattice parameters are given. These data re-

^{a)}Electronic mail: wenweige@vt.edu.

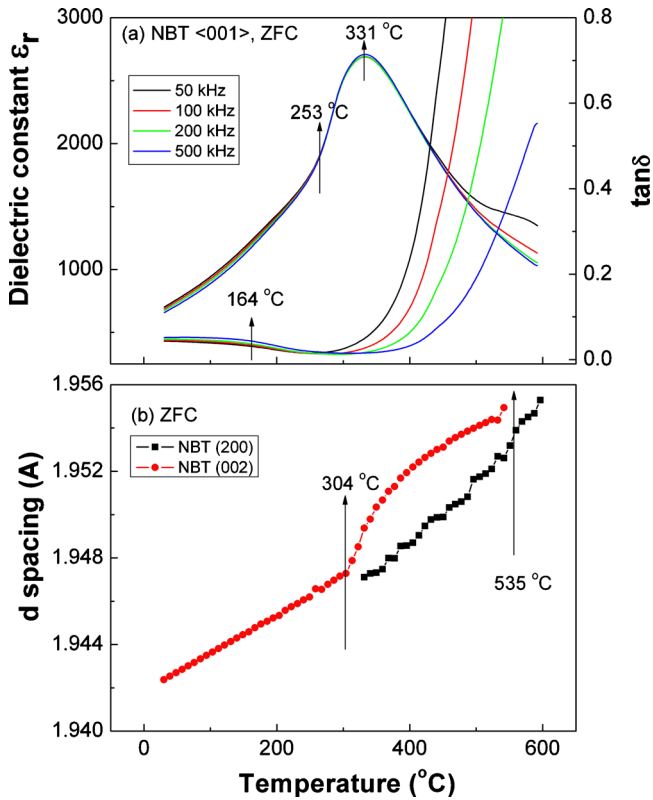


FIG. 1. (Color online) Phase transformation characteristics of (001) oriented NBT single crystal in the zero-field cooled condition, observed by (a) temperature dependent dielectric constant measurements taken at various frequencies; and (b) temperature dependent lattice parameter measurements.

veal a splitting of c and a parameters in the temperature range between 300 and 530 °C: demonstrating that both the polar (near and below T_{\max}) and prototypic ($>T_{\max}$) phases have tetragonal symmetry. Below 300 °C, the structure is transformed to rhombohedral (i.e., pseudocubic). No other structural changes were found at the Curie temperature, or at the inflection in the dielectric constant near 250 °C. These XRD results do not preclude that a structural phase transition occurred on a local scale in some regions of the crystal near or above T_{\max} . A diffuse phase transition is apparent in the broad dielectric response with a maximum near T_{\max} , consistent with this possibility. However, if such local $T \rightarrow R$ transitions occur, they have correlation lengths less than that of the coherence length of x-ray required by the optical diffraction conditions. Thus, they would not be detectable at the Bragg conditions.

Figure 2 shows PLM images taken at various temperatures: [(a) and (b)] 25 °C in the R phase; [(c) and (d)] 250 °C near the temperature at which frequency dispersion became evident in the dielectric constant; [(e) and (f)] close to but below T_{\max} at 325 °C; and [(g) and (h)] near but below the $T \rightarrow C$ transition at 500 °C. The angles (θ) provided in the images are that between the polarizer/analyzer (P/A) pair and the pseudocubic $\langle 110 \rangle$. The left column shows images at $\theta=0^\circ$, and the right one at $\theta=45^\circ$.

Fig. 2 clearly reveal the presence of tetragonal ferroelastic domains for temperatures below 500 °C, which have a width of about 10–100 μm and a length on the order of hundreds of microns, and which are oriented along the $\langle 110 \rangle$. These ferroelastic domains disappeared on heating at the $T \rightarrow C$ transition near 550 °C (data not shown). It is important

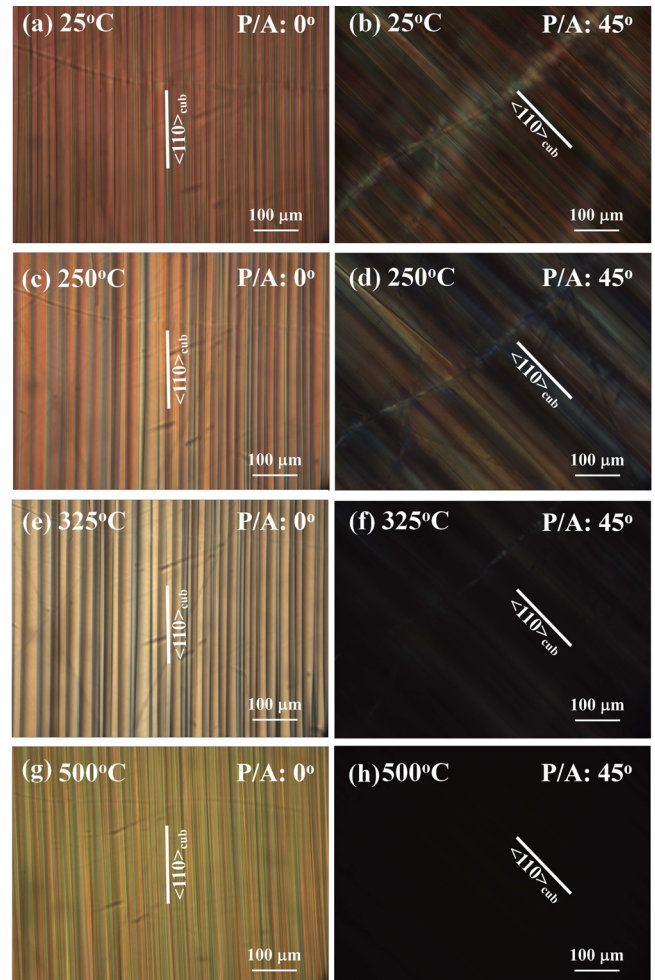


FIG. 2. (Color online) PLM images taken at various temperatures of [(a) and (b)] 25 °C, [(c) and (d)] 250 °C, [(e) and (f)] 325 °C, and [(g) and (h)] 500 °C, respectively.

to note that the size, shape, and position of these ferroelastic domains were somewhat unchanged with temperature on cooling between 500 °C and room temperature, even though the sample went through (i) two polar phase transformations on cooling, and (ii) that the ferroelastic tetragonal strain (c/a) disappeared at 300 °C on cooling into the R phase. These findings clearly demonstrate that the ferroelastic domain structure is inherited into the rhombohedral polar phase at room temperature.

Also, please note in Fig. 2 the extinction at different temperatures. At 550 °C, complete extinction was found for $\theta=0^\circ$ to 360° (data not shown): this indicates that NBT is cubic and optically isotropic as revealed by XRD data in Fig. 1(b). On cooling to 500 °C in the T phase field, ferroelastic domain appeared and the extinction angle was $\theta=45^\circ+m \times 90^\circ$ ($m=0, 1, 2,$ and 3): this is the typical extinction position for tetragonal structures. The extinction angle did not change on cooling to $T_{\max}=330^\circ\text{C}$ (data not shown). However, complete optical extinction could not be maintained on cooling to 325 °C [see Fig. 2(f)], even though NBT was still tetragonal by XRD. These results indicate that ferroelectric R phase nuclei have begun to form in the tetragonal matrix, as the R structure has extinction for $\theta=0^\circ$ rather than $\theta=45^\circ$. On cooling to and in the R phase field, the contrast in the extinction images for $\theta=45^\circ$ became more pronounced, as can be seen in Figs. 2(b) and 2(d); whereas the contrast in

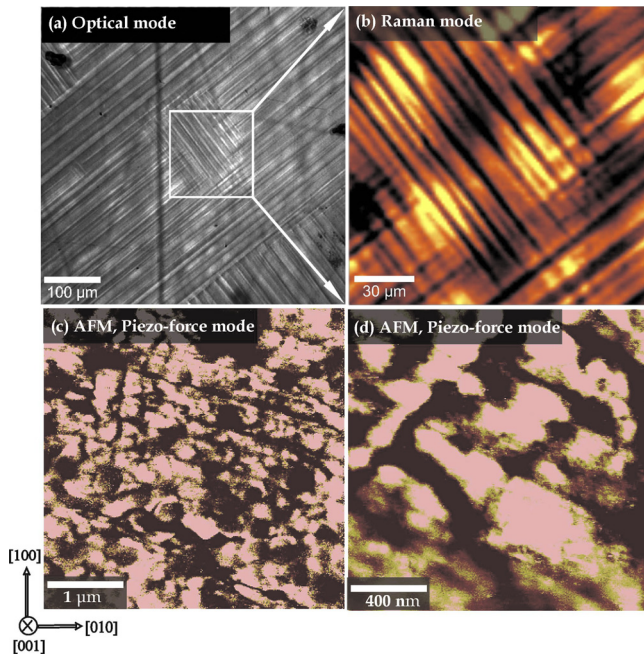


FIG. 3. (Color online) Domain structure of NBT at different length scales taken by (a) atomic force microscopy using an optical mode; (b) atomic force microscopy using a Raman mode, which demonstrates ferroelastic domains of about $10\ \mu\text{m}$; (c) atomic force microscopy, which shows ferroelectric domains of about $0.2\text{--}0.5\ \mu\text{m}$ in size; and (d) a higher resolution image of ferroelectric domains, which demonstrates much clear ferroelectric domains that exists within side the ferroelastic ones.

the images for $\theta=0^\circ$ also became darker on cooling between 325 to 25°C . Comparisons of the PLM images at various temperatures show that the optical extinction conditions gradually change with decreasing temperature below T_{max} . However, complete optical extinction could not be achieved in the R phase field. This indicates that the ferroelectric R domains in NBT crystals could not organize into large domain platelets or bands, as previously reported for PMN-PT crystals.^{14,15} These results clearly illustrate the diffused nature of the phase transformation, and that polar R nuclei initially begin to form near T_{max} .

Finally, we have performed investigations of the domain structure of NBT over various length scales using different types of microscopy. These investigations have shown the presence of two different types of domain structures of different characteristic sizes. We confirmed the presence of ferroelastic domains by optical mode and Raman mode SPM as shown in Figs. 3(a) and 3(b). In this case, $\langle 110 \rangle$ oriented domains of width about $10\ \mu\text{m}$ were found, consistent with the PLM images (see Fig. 2). We then performed SPM investigations using the piezoforce mode, so that we could detect the ferroelectric domain structure. Figures 3(c) and 3(d) show typical PFM images, which reveal the presence of much smaller ferroelectric domains that exist within the ferroelastic domains of larger length scale. The size of these ferroelectric domains was on the order of 0.2 to $0.5\ \mu\text{m}$. Furthermore, the spatial distribution of these ferroelectric microdomains was not well organized; however, comprehensive studies by PFM showed that the ferroelectric domains had some tendency for organization along the $\langle 110 \rangle$ direction.

Generally in a distortive phase transformation, changes in the domain variant distribution and population allow the

achievement of the elastic compatibility conditions and minimization of the elastic free energy.²⁰ However, our findings show a unique sequence of phase transformations in NBT, where a ferroelastic T domain structure is inherited into a ferroelectric R phase. This is important because it means that the polar R phase is geometrically and elastically restricted by its high temperature ferroelastic T parent phase. On cooling into the R phase, ferroelectric microdomains then form within the ferroelastic T domains. The system can organize the ferroelectric microdomain distribution in an attempt to achieve the invariant plane strain conditions; however, a fully relaxed elastic state is clearly not achieved for NBT. Because complete stress accommodation is not achieved, the polar microdomain ensemble may undergo low frequency dynamical fluctuations, typical of a relaxor ferroelectric state.

In summary, phase transformation and domain studies of NBT have revealed (i) that a high-temperature tetragonal ferroelastic domain structure is elastically inherited into a lower temperature rhombohedral ferroelectric phase; and (ii) that polar microdomains form within this geometrical constraint on cooling, resulting in a metastable state with attributes of a relaxor ferroelectric.

This work was financially supported by the National Science Foundation (Materials world network) under Grant No. DMR-0806592, by the Department of Energy under Grant No. DE-FG02-07ER46480, by the National Science Foundation of China under Grant No. 50602047, and by the Shanghai Municipal Government under Grant No. 08JC1420500.

¹T. Takenaka, K. Maruyama, and K. Sakata, *Jpn. J. Appl. Phys., Part 2* **30**, 2236 (1991).

²Y. M. Chiang, G. W. Farrey, and A. N. Soukhovjak, *Appl. Phys. Lett.* **73**, 3683 (1998).

³G. Smolenskii, V. Isupov, A. Agranovskaya, and N. Kainik, *Sov. Phys. Solid State* **2**, 2651 (1961).

⁴Q. Zhang, Y. Zhang, F. Wang, Y. Wang, D. Lin, X. Zhao, H. Luo, W. Ge, and D. Viehland, *Appl. Phys. Lett.* **95**, 102904 (2009).

⁵J. Zvirzdzs, P. Kapostin, J. Zvirgzde, and T. Kruzina, *Ferroelectrics* **40**, 75 (1982).

⁶S. Vakhrušev, V. Isupov, B. Kvyathkovsky, N. Okeuneva, I. Pronin, G. Smolensky, and P. Syrnikov, *Ferroelectrics* **63**, 153 (1985).

⁷J. Suchanicz and J. Kwapulinski, *Ferroelectrics* **165**, 249 (1995).

⁸J. Kusz, J. Suchanicz, H. Bohm, and J. Warzewski, *J. Phase Trans.* **70**, 223 (1999).

⁹G. Jones and P. Thomas, *Acta Crystallogr., Sect. B: Struct. Sci.* **B58**, 168 (2002).

¹⁰K. Hong and S. Park, *J. Appl. Phys.* **79**, 388 (1996).

¹¹V. Dorcet, G. Trolliard, and P. Boullay, *Chem. Mater.* **20**, 5061 (2008).

¹²I. Pronin, P. Syrnikov, V. Isupov, and G. Smolenskii, *Sov. Tech. Phys. Lett.* **8**, 563 (1982).

¹³Z. Xu, M. C. Kim, J.-F. Li, and D. Viehland, *Philos. Mag. A* **74**, 395 (1996).

¹⁴F. Bai, J. F. Li, and D. Viehland, *Appl. Phys. Lett.* **85**, 2313 (2004).

¹⁵F. Bai, J. F. Li, and D. Viehland, *J. Appl. Phys.* **97**, 054103 (2005).

¹⁶V. I. Syutkina and E. S. Jakovleva, *Phys. Status Solidi* **21**, 465 (1967).

¹⁷Y. Jin, Y. Wang, A. Khachatryan, J. F. Li, and D. Viehland, *Phys. Rev. Lett.* **91**, 197601 (2003).

¹⁸W. Ge, H. Liu, X. Zhao, X. Pan, T. He, D. Lin, H. Xu, and H. Luo, *J. Alloys Compd.* **456**, 503 (2008).

¹⁹D. Viehland, S. Jang, L. Cross, and M. Wuttig, *J. Appl. Phys.* **68**, 2916 (1990).

²⁰A. B. Kouna Njiwa, E. Aulbach, T. Granzow, and J. Rödel, *Acta Mater.* **55**, 675 (2007).